Author Accepted Manuscript version of the paper by Andres A. Valdez-Fernandez et al. in 2023 International Symposium on Electromobility - ISEM (2023) Page,
DOI: http://dx.doi.org/10.1109/ISEM59023.2023.10334918

A model-based controller for an isolated inverter for electric vehicle applications

Andres A. Valdez-Fernandez
Eduardo A. Gutierrez-Robles
School of Sciences, UASLP
San Luis Potosi, Mexico
email: [andres.valdez, eduardo.alejandrogt]@ieee.org

Gerardo Escobar
School of Engineering and Sciences
Tecnologico de Monterrey
Monterrey, Mexico
email: gerardo.escobar@tec.mx

Raymundo E. Torres-Olguin
Dept. Energy Systems
SINTEF energy
Trondheim, Norway
email: raymundo.torres-olguin@sintef.no

***Abstract*—This paper proposes a model-based controller for a state-of-the-art isolated inverter, with the aim to provide a low THD true-sine wave (TSW) single-phase voltage to feed auxiliary loads in EV applications, which is a requirement of great relevance in the current market. The studied topology comprises two stages, namely an isolated DC-DC converter, and a TSW inverter. Isolation in the first stage is provided by means of a high-frequency transformer fed by an H-bridge converter, which creates a high-frequency switching alternating signal out of the EV DC-bus voltage. The transformer output is processed by a full-bridge rectifier and a filter to create a regulated DC voltage signal. In the second stage, an H-bridge converter followed by a second-order filter creates a TSW by inverting the regulated DC output of the DC-DC converter. The proposed controller comprises a proportional-integral-derivative (PID) solution to regulate the DC output voltage of the DC-DC isolated converter; and a proportional-resonant (PR) solution to guarantee a TSW output voltage with low THD in spite of the presence of non-linear distorting loads. In particular, the PR controller involves the measurement of the output capacitor current to incorporate additional damping. Simulation results are presented to assess the performance of the proposed control algorithms.**

***Index Terms*—True-sine wave inverter, electric vehicle, DC-DC converter, isolated converter, galvanic isolation**

I. Introduction

Users of electric vehicles (EV) connect a variety of electrical devices referred to as auxiliary loads, such as smartphone chargers, video game consoles, computers, work tools, and among others. Normally, these auxiliary loads are of a non-linear nature,i.e. they produce distorting currents with high total harmonic distortion (THD) [1], containing, for instance, odd harmonics of the fundamental frequency. Therefore, the auxiliary loads may cause problems inside the vehicle system, such as voltage distortion, electromagnetic interference, harmonic resonances, and even a decrease in the overall system efficiency [2].

In high DC-voltage applications of electric vehicles (EVs), robust protections are essential for both devices and users, especially because EV systems involve power and signal lines, and any interference between them could have serious conseuqeunces [3]. Guarantee of galvanic isolation between the charging supply, the electric road systems and the on-board battery circuit in the vehicle is of great relevance [4]. Power converters with galvanic isolation are widely used in various applications and are a must in industry safety standards (e.g., IEC60950 and UL2202) [5]. In general, galvanic isolation (with power transmission) can be achieved using piezoelectric, dielectric or magnetic elements. Magnetic isolation is perhaps the most common method for achieving galvanic isolation and is carried out using a transformer. Unlike its alternatives, it has no power transfer limitations, and it is smaller than dielectric methods [6].

The power electronics community offers multiple ways to guarantee isolation in electrical systems, for instance, using a high-frequency transformer (pulse transformer) to create a so-called isolated high-frequency DC-DC converter, which is one of the most widely used solutions [7]. The need for isolation restricts the available DC-DC topologies to those involving a high-frequency transformer [8]–[10]. Therefore, some traditional topologies, like flyback, forward and push-pull converters, are not suitable for this application as the involved transformer (in some cases rather a coupled inductance) is larger [8]. In contrast, the dual active bridge (DAB) topology is one of the most used topologies for bidirectional, high power and high voltage gain applications, it is formed by two full-bridge converters connected through a transformer [9]. However, in the particular application of auxiliary loads in EV, the power flow is unidirectional and the H-bridge converter connected to the high-frequency transformer of a DAB topology can be replaced by a simple full-bridge diode-based rectifier [10].

The obtained DC voltage generated by the isolated DC-DC converter can be inverted to power particular loads requiring an AC supply. Most practical inverters may generate a periodic signal not precisely of perfect sinusoidal waveform but containing a certain amount of harmonic distortion [11]. A figure of merit regularly used to measure the quality of the output voltage is the total harmonic distortion (THD), which must be kept as small as possible [12] to guarantee an output signal as close as possible to a sinusoidal. The inverters used to supply auxiliary loads can be classified as modified-sine wave (MSW) and true-sine wave (TSW). An MSW inverter generates a square wave output voltage or a quasi-square wave voltage. These types of waveforms comprise undesirable

Author Accepted Manuscript version of the paper by Andres A. Valdez-Fernandez et al. in 2023 International Symposium on Electromobility - ISEM (2023) Page,
DOI: http://dx.doi.org/10.1109/ISEM59023.2023.10334918

harmonics and consequently a high THD, which makes them not suitable for sensitive electrical devices [13]. TSW inverters have significantly less harmonic content than MSW inverters, resulting in a smaller THD than MSW topologies. Different TSW inverter topologies have been studied in the literature, for instance, the full bridge inverter, a high-frequency transformer plus an AC-DC-AC rectifier-inverter [10], matrix converters [14], etc.

The present work proposes a model-based controller for a state-of-the-art isolated inverter, with the aim to provide a low THD TSW single-phase voltage to feed auxiliary loads in EV applications. The isolated inverter consists of two cascade-connected stages namely an isolated high-frequency DC-DC converter, and a TSW inverter (see Fig. 1). The proposed controller comprises a proportional-integral-derivative (PID) solution to regulate the DC output voltage of the DC-DC isolated converter; and a proportional-resonant (PR) solution to guarantee a TSW output voltage with low THD in spite of the presence of non-linear distorting loads. In particular, the PR controller involves the measurement of the output capacitor current to incorporate additional damping. Simulation results are included to show that, under the proposed control algorithm, the DC output of the DC-DC converter can be regulated, while a TSW output voltage can be obtained with a low THD despite the connection of a non-linear auxiliary load.

The rest of the paper is organised as follows: Section 2 provides a system description of the inverter and the controllers used to achieve the desired output voltage. Section 3 provides the principles of the modulation schemes used for the two H-bridge inverters involved. Section 4 provides the numerical evaluation of the proposed scheme under different test conditions. Section 5 provides concluding remarks on the research work.

II. System description

Figure 1 shows the circuit diagram of the studied topology referred to as the isolated inverter, which comprises an isolated DC-DC converter and a TSW inverter to supply auxiliary loads with an AC signal. The isolated DC-DC converter is composed of the cascade connection of a full-bridge DC-DC converter that creates a high-frequency oscillating voltage signal, a high-frequency transformer to ensure galvanic isolation, a diode-bridge rectifier to rectify the high-frequency oscillating signal, and a second-order filter L_bC_b to reduce the switching ripple. The result is an almost constant voltage-regulated signal v_{Cb}. As above mentioned, some loads in an EV must operate with an AC power supply at a given amplitude and relatively low frequency. To provide such a low frequency almost sinusoidal signal, an inverter plus a second order filter LC, as the one shown in Fig. 1, have been attached to the output regulated voltage of the isolated DC-DC converter to create and deliver the required AC signal out of the v_{Cb}. Moreover, the inverter must provide an almost pure sinusoidal (also referred to as TSW) whose characteristics of magnitude and frequency are preserved despite the connection of auxiliary distorting nonlinear loads.

A. Mathematical model

The mathematical model describing the dynamics of the galvanically *isolated DC-DC converter* (first stage) is given by

$$L_b\frac{di_{Lb}}{dt} = -r_b i_{Lb} - v_{Cb} + e_b, \quad e_b \triangleq (1-d_b)E \tag{1}$$

$$C_b\frac{dv_{Cb}}{dt} = i_{Lb} - i_{0b} = i_{Cb} \tag{2}$$

where L_b and C_b are the inductance and capacitance, respectively (subindex b comes from the bridge); r_b is the inductor parasitic resistance; E is the voltage of the EV DC-link, v_{Cb} is the capacitor voltage, i_{Lb} is the inductor current (or the bridge rectifier output current), i_{0b} is the converter output filtered current (or the demanded current of the *TSW inverter*); $0{\leq}d_b{\leq}1$ is the duty-cycle of a modulation scheme, for instance, a *single-pulse width modulation* (single-PWM) scheme, used to generate the switching sequence, and represents the actual control input of the isolated DC-DC converter. It is worth noticing that, an average model has already been considered under the assumption of a relatively high switching frequency with respect to the cutoff frequency of the LPF operation of the attached second-order filter conformed by L_bC_b.

The mathematical model describing the dynamics of the *TSW inverter* (second stage) is given by

$$L\frac{di_L}{dt} = -ri_L - v_0 + e, \quad e \triangleq dv_{Cb} \tag{3}$$

$$C\frac{dv_0}{dt} = i_L - i_0 = i_C \tag{4}$$

where L and C are the inductance and capacitance of the filter LC, respectively; r is the inductor parasitic resistance; i_L, i_C are the inductor and capacitor currents, respectively; v_0 is the output capacitor voltage; and i_0 is the current demanded by the non linear load. Moreover, $-1{\leq}d{\leq}1$ represents the duty-cycle used in a modulation scheme, for instance, a *sinusoidal-pulse width modulation* (SPWM) scheme, to recover the switching sequence, and plays the role of the actual control input in the TSW inverter. Same as for the isolated DC-DC converter, it is worth noticing that, an average model has already been considered under the assumption of a relatively high switching frequency, and an LPF operation of the attached second order filter conformed by L and C.

B. Control objectives

The main control objective of the *isolation stage* consists of designing a control signal e_b (or equivalently d_b) to regulate the capacitor voltage v_C towards a constant reference V_d, i.e.,

$$v_{Cb} \to V_d, \quad t \to \infty \tag{5}$$

The main control objective for the *inverter stage* consists in designing a control signal e (or equivalently d) to guarantee a TSW voltage in the inverter output voltage v_0 despite a distorting load current i_0; in other words, v_0 is forced to track a purely sinusoidal reference signal v_0^*, that is,

$$v_0 \to v_0^* = V_p \sin(\omega_0 t), \quad t \to \infty \tag{6}$$

where ω_0 ($\omega_0 = 2\pi f_0$) is the fundamental frequency.

Author Accepted Manuscript version of the paper by Andres A. Valdez-Fernandez et al. in 2023 International Symposium on Electromobility - ISEM (2023) Page,
DOI: http://dx.doi.org/10.1109/ISEM59023.2023.10334918

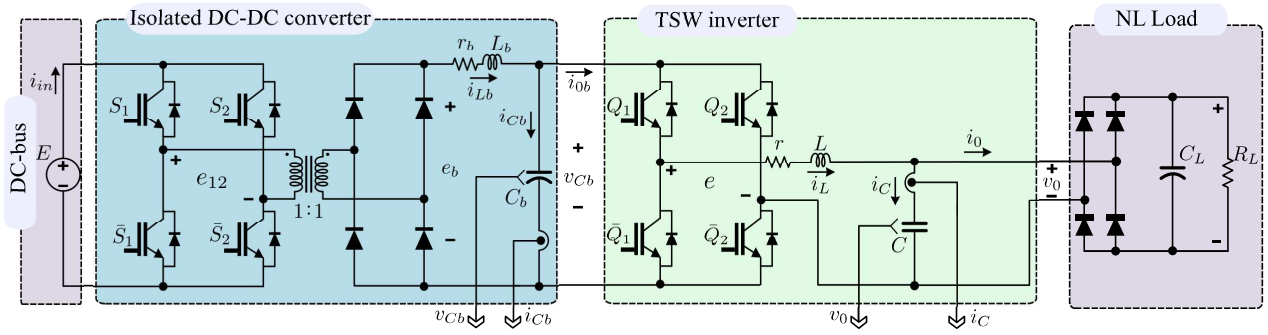

Fig. 1. Isolated inverter to feed AC auxiliary loads in electric vehicle applications

C. Main assumptions

The following assumptions are considered to restrict and facilitate the solution of the control objectives:

- **A1**. Filter parameters L_b, C_b, r_b, L, C, r are unknown constants.
- **A2**. EV DC-bus voltage E is a known constant.
- **A3**. Variables v_{Cb}, i_{Cb}, v_0, and i_C are available from measurements.
- **A4**. The output voltage of the isolated converter is bounded away from zero, i.e., $v_{Cb} > 0$.
- **A5**. The load current is a periodic signal containing mainly odd harmonics, that is, harmonics in the set $\mathcal{H} = \{1, 3, 5, \dots\}$

III. Controller Design

Notice that, after the definition of the new control variable $e = dv_{Cb}$, and assuming that $v_{Cb} > 0$, both systems (1)-(2) and (3)-(4) become decoupled from each other, and thus the control design can also be split in two loops, namely the *isolation stage* and the *inverter stage*, which enormously simplifies the design, as described in what follows.

A. Isolation stage

The systems dynamics (1)-(2) can be rewritten, in terms of the capacitor current i_{Cb} and the voltage increment $\tilde{v}_{Cb} \triangleq v_{Cb} - V_d$, as follows:

$$L_b \frac{di_{Cb}}{dt} = -r_b i_{Cb} - \tilde{v}_{Cb} + e_b - \phi_b \tag{7}$$

$$C_b \frac{d\tilde{v}_{Cb}}{dt} = i_{Cb} \tag{8}$$

where ϕ_b represent a perturbation given by $\phi_b = V_d + r_i i_{0b} + L_C di_{0b}/dt$. Notice that ϕ_b can be rewritten as the sum of a DC and AC components, i.e., $\phi_b = \langle\phi_b\rangle_{DC} + \langle\phi_b\rangle_{AC}$, with $\langle\phi_b\rangle_{DC} = V_d + r_b\langle i_{0b}\rangle_{DC} > 0$, and $\langle\phi_b\rangle_{AC} = r_i\langle i_{0b}\rangle_{AC} + L_C d\langle i_{0b}\rangle_{AC}/dt$. That is, system (7)-(8) turns out to be a controllable second-order linear time-invariant system perturbed by a biased oscillating disturbance ϕ_b. Following the ideas of the *energy shaping plus damping injection* design technique [15], the following PID controller is proposed to guarantee that $\tilde{v}_{Cb} \to 0$ (or equivalently, regulation of $v_{Cb} \to V_d$):

$$e_b = -k_p \tilde{v}_{Cb} - k_i \int \tilde{v}_{Cb} dt - k_d i_{Cb} \tag{9}$$

where $k_p > 0$ and $k_d > 0$ are design parameters to add damping and $k_i > 0$ is the integral gain. Notice that, based on (8), the derivative part is performed using the measurement of capacitor current i_{Cb} instead of calculating the time derivative of the capacitor voltage, which may lead to noise issues. Notice also that this controller can only guarantee regulation of v_{Cb} in average, that is, a small amount of ripple in v_{Cb} is expected due to the AC perturbation $\langle\phi_b\rangle_{AC}$.

B. Inverter stage

A voltage controller is proposed for the single-phase TSW inverter based on feedback variables v_0 and i_C. As it will become clear later, the required damping is introduced through the feedback of i_C, which is assumed available from measurements. For design purposes, it is convenient to express the system dynamics (3)-(4) in terms of the increments $\tilde{v}_0 \triangleq v_0 - v_0^*$ and $\tilde{i}_C \triangleq i_C - i_C^*$ as follows:

$$L \frac{d\tilde{i}_C}{dt} = -\tilde{v}_0 - r\tilde{i}_C + e - v_0^* - \phi \tag{10}$$

$$C \frac{d\tilde{v}_0}{dt} = \tilde{i}_C \tag{11}$$

where $i_C^* = C dv_0^*/dt$ is the steady state response of i_C, and $\phi \triangleq r(i_0 + i_C^*) + Ld(i_0 + i_C^*)/dt$ represents a periodic disturbance. Notice that the *matching condition* is met in system (10)-(11), i.e., the disturbance ϕ appears in the same subsystem (row) as the control signal e. Therefore, the following proportional plus resonant (PR) controller based on the *internal model principle* is proposed as an appropriate solution to guarantee perfect tracking, i.e. $\tilde{v}_0 \to 0$:

$$e = -k_1 i_C - (k_2 + 2\sum \gamma_k)\tilde{v}_0 + v_0^* + \\ + \sum_{k \in \mathcal{H}} \frac{2\gamma_k k^2 \omega_0^2}{s^2 + k^2\omega_0^2} \tilde{v}_0 \tag{12}$$

where k_1 and k_2 are two positive design parameters to add the required damping; and $\gamma_k > 0$ is the gain of the kth resonant filter to compensate the kth harmonic in the set $\mathcal{H}$ that includes all the odd harmonics generated by the nonlinear load. This

Author Accepted Manuscript version of the paper by Andres A. Valdez-Fernandez et al. in 2023 International Symposium on Electromobility - ISEM (2023) Page,
DOI: http://dx.doi.org/10.1109/ISEM59023.2023.10334918

controller also guarantees that $\tilde{i}_C \to 0$, although this is not the main objective.

Figure 2 shows the controller previously discussed for both the regulation in the isolated DC-DC converter and the tracking in the TSW inverter. Notice that, in contrast to conventional PR controllers, the resonant filters generate the quadrature component, i.e., there is not a derivative effect in the numerator (zero in the origin).

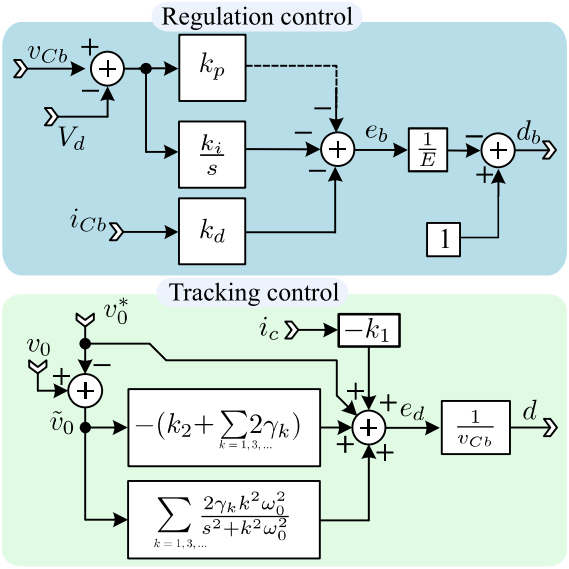

Fig. 2. Controller scheme used to solve both the regulation in the isolated DC-DC converter and the tracking in the TSW inverter.

IV. Modulation Schemes

This section describes the modulation techniques used to recuperate the corresponding switching sequences for both the isolated DC-DC converter and the TSW inverter. It is noteworthy that both schemes require different modulation schemes, although both are based on the conventional PWM.

Table I shows the output voltage of the full bridge inverter e_{12} out of the permissible combinations of switches S_1, $\bar{S}_1$,S_2, $\bar{S}_2$, and assuming a constant input voltage E on the DC-bus of the EV.

TABLE I
Inverter voltage e_{12} generated out of the switching states permissible combinations.

S_1	$\bar{S}_1$	S_2	$\bar{S}_2$	e_{12}
ON	ON	OFF	OFF	E
ON	OFF	ON	OFF	0^+
OFF	ON	OFF	ON	0^-
OFF	OFF	ON	ON	-E

For the isolated DC-DC converter a *single-PWM* scheme is selected. In this scheme the control signal $\bar{d}_b \triangleq (1-d_b)$ is compared against the alternating triangular carrier signals f_{saw} and $\bar{f}_{saw}$, where $\bar{d}_b$ is the complement of the duty-ratio d_b, as $0 \leq d_b \leq 1$, and $\bar{f}_{saw} = -f_{saw}$. The comparison of $\bar{d}_b$ against f_{saw} generates the switching signals S_1 and its complementary $\bar{S}_1$, while the comparison of $\bar{d}_b$ against $\bar{f}_{saw}$ delivers S_2 and $\bar{S}_2$. For instance, if $\bar{d}_b < f_{saw}$, then S_1 turns on ($\bar{S}_1$ turns off), and vice versa. In this type of modulation, there is only one pulse per period on each branch, each pulsating signal is phase-shifted by half a period with respect to each other. Therefore, an alternate pulsating signal is generated between the two branches given by $e_{12} = (S_1 - S_2)E$. Moreover, the pulse width in both pulsating signals S_1 and S_2 is proportional to $\bar{d}_b$, which is the mechanism to control the average of the amplitude of the composed switching signal e_{12}. This technique is usually intended for high-frequency applications. In fact, the effective frequency of the inverter output voltage e_{12} is twice the frequency of the triangular carrier signals f_{saw} and $\bar{f}_{saw}$. Figure 3 shows the waveforms generated with the single-PWM scheme, where a duty cycle of $d_b = 0.4$ has been selected, the frequency for the carriers is fixed to 10 kHz, and an input voltage $E = 200$ V on the DC-bus has been considered.

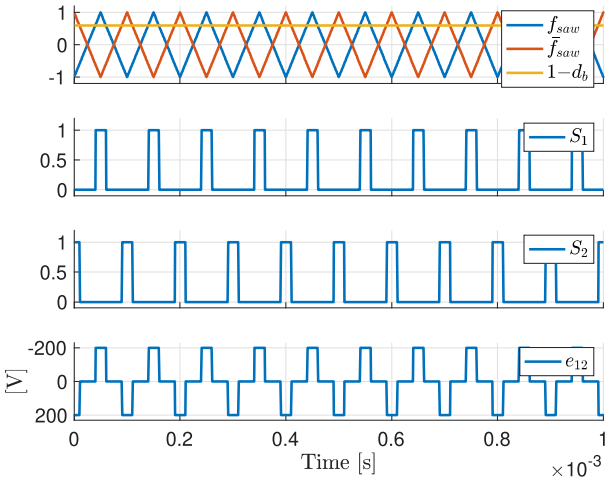

Fig. 3. (From top to bottom) Comparison between the control signal $\bar{d}_b \triangleq (1-d_b)$ and the triangular carrier signals f_{saw} and $\bar{f}_{saw}$; switching signal S_1; switching signal S_2; and inverter switching output voltage $e_{12} = (S_1 - S_2)E$.

For the TSW inverter, a *SPWM* scheme has been considered to realize a unipolar modulation, which is a quite common technique to produce an almost sinusoidal waveform out of a full-bridge inverter plus a filtering process [7]. In this modulation technique the control signal d $(-1 \leq d \leq 1)$ is compared against two carrier signals g_{saw} and $\bar{g}_{saw}$, where $\bar{g}_{saw} = -g_{saw}$, as usual in the unipolar modulation. The switching policy for the first branch is defined as follows: if $d > g_{saw}$, then Q_1 turns on ($\bar{Q}_1$ turns off), and vice versa; while, for the second branch if $d > \bar{g}_{saw}$, then Q_2 turns on ($\bar{Q}_2$ turns off), and vice versa. The resulting output signal measured between both branches is given by $e = (Q_1 - Q_2)v_{Cb}$. Unlike single-PWM, the fundamental frequency of the output voltage is determined by the frequency of the modulation signal, while the effective switching frequency is twice the switching frequency of the switching devices. Figure 4 shows

Author Accepted Manuscript version of the paper by Andres A. Valdez-Fernandez et al. in 2023 International Symposium on Electromobility - ISEM (2023) Page,
DOI: http://dx.doi.org/10.1109/ISEM59023.2023.10334918

the waveforms generated by the SPWM scheme, where a switching frequency of 500 Hz has been selected only for demonstration purposes, which corresponds to an effective frequency of 1 kHz observed at e; and a sinusoidal reference signal with unitary modulation index is used as an example.

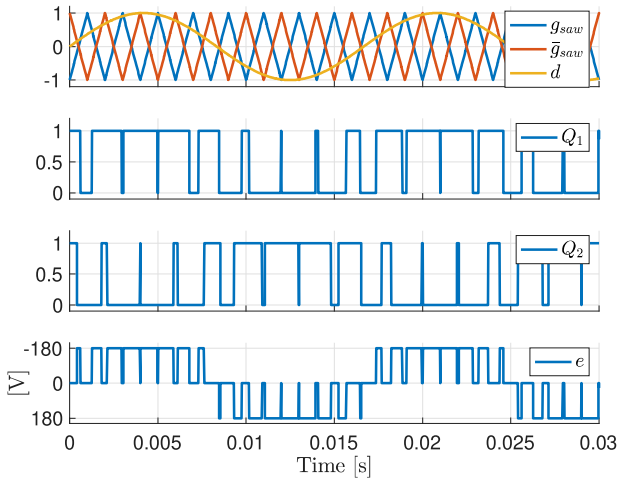

Fig. 4. (From top to bottom) Comparison between the modulation signal d and the triangular carrier signals g_{saw} and $\bar{g}_{saw}$; switching signal Q_1; switching signal Q_2; and inverter switching output voltage e=$(Q_1-Q_2)v_{Cb}$.

V. Numerical Results

The system shown in Fig. 1 was evaluated in PSIM considering 1 μs of time step and a total time of 600 ms. The simulation considered the following parameters: (for the isolated DC-DC converter) L_b = 0.17 mH, C_b = 540 μF, r_b = 0.1 Ω, DC-bus voltage E = 210 V, switching frequency $f_{sw,b}$ = 33 kHz, and capacitor voltage reference V_d = 180 V; (for the TSW inverter) L = 1 mH, C = 20 μF, switching frequency f_{sw} = 10 kHz and reference for the output voltage (peak) amplitude V_p = 180 V. The non-linear load (connected to the inverter output) comprised a diode bridge rectifier with a filter capacitor C_L = 62 μF feeding a resistor R_L. The value of this latter fluctuates between 50 Ω and 100 Ω to test the performance under load step changes. The weights α_1 and α_2, used to create i_g, were set to 10 and 1, respectively. The results were processed and displayed using Matlab.

The control parameters are fixed as follows. For the isolation stage: $k_p = 3$, $k_i = 3$, $k_d = 0.01$, $V_d = 180$ V. For the inverter stage: $k_1 = 40$, $k_2 = 40$, $\gamma_1 = 0.1$, $\gamma_3 = 0.08$, $\gamma_5 = 0.5$, $\gamma_7 = \gamma_9 = 0.3$, $\gamma_{11} = 0.1$, $\gamma_{13} = 0.08$, $V_p = 180$ V. Figure 5 shows the transient responses of (from top to bottom) the input current i_{in} taken from the EV DC-bus; the output power P_0 demanded by the non-linear load, i.e., the DC component of the instantaneous power $p_0 = v_0 \times i_0$; and the isolated DC-DC converter output voltage v_{Cb} and its reference V_d; for the isolated inverter under the proposed controller, during the start-up operation and during load step changes. For this latter, R_L changes from 50 Ω to 100 Ω and back. As expected, the amplitude of the input current i_{in} changes accordingly. It can be observed that, during the start-up, the voltage v_{Cb} achieves its reference V_d=180 V after a relatively small transient, and then it maintains (on average) its value around the reference despite the load changes.

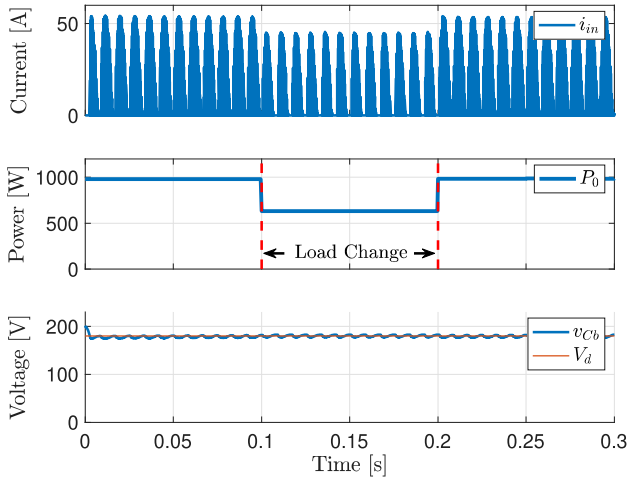

Fig. 5. Transient responses, under the proposed controller and during load step changes (R_L goes from 50 Ω to 100 Ω and back), of (from top to bottom) the input current i_{in} taken from the EV DC-bus, the output power P_0 demanded by the non-linear load, and (bottom) the isolated DC-DC converter output voltage v_{Cb} (in blue) and its reference V_d (in red).

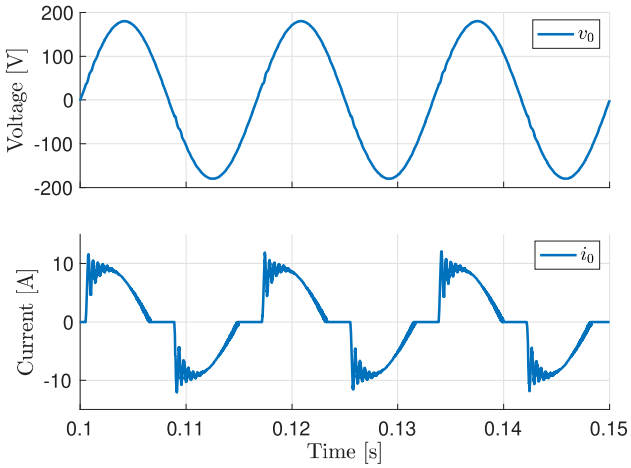

Fig. 6. Steady state responses, under the proposed controller, of (top) the TSW inverter output voltage v_0, and (bottom) the output current i_0 generated by the non-linear load.

Figure 6 shows, under the proposed controller, the steady-state responses of (top) the TSW inverter output voltage v_0, and (bottom) the output current i_0 generated by the nonlinear load. As observed, the voltage v_0 has a TSW shape, which corresponds to a THD = 1.42% despite the nonlinear load connected to the inverter having a THD of about 32%. It is worth noticing that the voltage v_0 undergoes a small deformation as a consequence of the drastic change in the shape of the load current.

Figure 7 shows the frequency spectra of (top) the TSW inverter output voltage v_0, and (bottom) the output current i_0

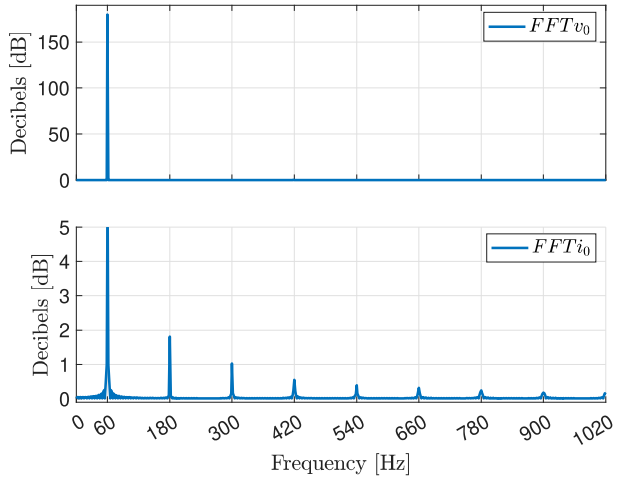

Fig. 7. (Top) $FFTv_0$, (bottom) $FFTi_0$.

generated by the nonlinear load. Notice that the odd harmonics present in the frequency spectrum of i_0 do not propagate to v_0 due to the excellent harmonic compensation performed by the bank of resonant filters, leading to an output voltage composed mainly by a fundamental component with a THD $= 1.42\%$ despite the harmonics generated by the load.

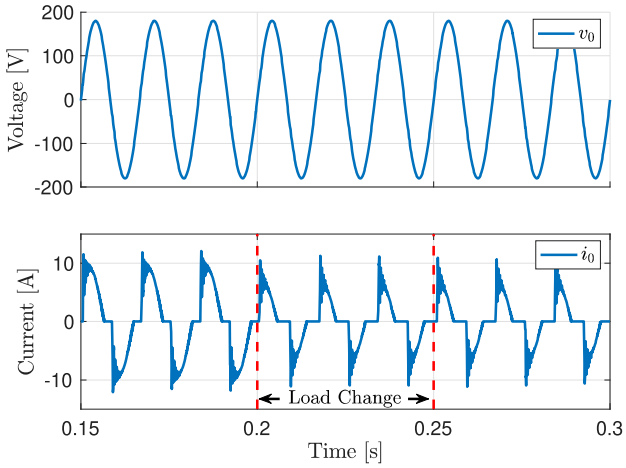

Fig. 8. Transient responses, under the proposed controller and during a load step change (R_L goes from 50 Ω to 100 Ω and back), of (Top) the TSW inverter output voltage v_0, and (bottom) output current i_0 generated by the non-linear load.

Figure 8 shows (top) the transient response of the TSW inverter output voltage v_0 and (bottom) the load current i_0 under load step changes, where R_L goes from 50 Ω to 100 Ω and back. Notice that, regardless of the harmonic contents and step changes in the load current i_0, the output voltage v_0 maintains the desired sinusoidal shape and amplitude.

Figure 9 shows the steady state response, under the proposed controller, of (from top to bottom) the reference voltage v_0^*, the TSW inverter output voltage v_0, and the tracking error $\tilde{v}_0$. Notice that the voltage v_0 has an almost purely

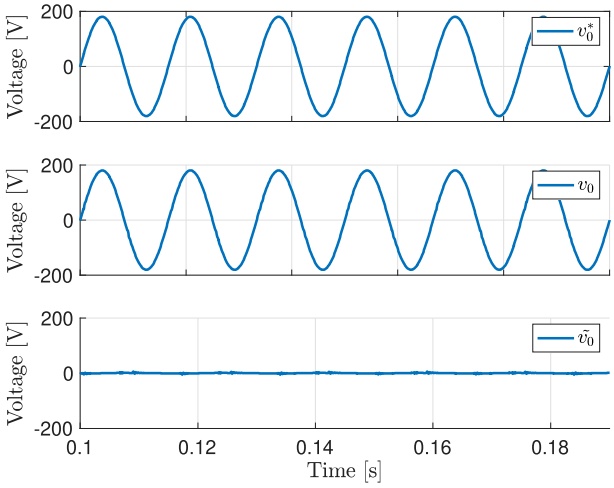

Fig. 9. Steady state responses, under the proposed controller, of (from top to bottom) the sinusoidal voltage reference v_0^*, the output voltage v_0, and the tracking error $\tilde{v}_0$.

sinusoidal waveform, keeping an excellent tracking to v_0^*, as a consequence, the tracking error $\tilde{v}_0 \approx 0$.

VI. Conclusion

This work presented the generalized modeling and the controller design for an isolated inverter used to feed auxiliary loads in electric vehicle applications. The studied isolated inverter comprises two stages, namely a DC-DC isolated converter (isolation stage) and a true sine waveform inverter (inverter stage). On the one hand, the isolation stage used a full-bridge inverter, a transformer to achieve galvanic isolation and a second-order (LC circuit) low-pass filter. The output of such an isolated DC-DC converter was regulated by modulating the width of the switching pulses on the full-bridge inverter and controlled by means of a PI controller. On the other hand, the inverter stage consisted of a full-bridge active inverter using an SPWM modulation scheme, where the switching harmonics were filtered out by a second-order (LC circuit) LPF. The reference for the SPWM scheme, corresponding to the average control signal was able to guarantee excellent tracking towards a TSW reference, with compensation of harmonic distortion. This controller used capacitor current measurements to add the required damping. Simulation results were presented to assess the performance of the isolated inverter under the proposed controller, that is, to demonstrate an almost perfect tracking towards a sinusoidal output voltage reference signal plus the harmonic compensation provided by the bank of resonant filters, while keeping all internal signals bounded.

References

[1] A. Ulinuha and E. Sari, "The influence of harmonic distortion on losses and efficiency of three-phase distribution transformer," Journal of Physics: Conference Series, vol. 1858, p. 012084, 04 2021.

[2] M.J.H. Rawa, D.W.P. Thomas, and M. Sumner, "Simulation of non-linear loads for harmonic studies," in *Proc. IEEE EPQU*, Oct. 17–19, 2011, pp. 1–6.

[3] G. Rajendran, C.A. Vaithilingam, N. Misron, K. Naidu and M.R. Ahmed, "Voltage Oriented Controller Based Vienna Rectifier for Electric Vehicle Charging Stations," *IEEE Access*, vol. 9, pp. 50798-50809, 2021.
[4] A. Karlsson and M. Alaküla, "Integrated and isolated EV charger for AC and Electric Road applications," in *Proc. IEEE SPEEDAM*, June 26–24, 2020, pp. 114-119.
[5] Y. Zhang, et.al., "Development of a WBG-based Transformerless Electric Vehicle Charger with Semiconductor Isolation," in *IEEE SPEC*, Dec. 10–13, 2018, pp. 1-6.
[6] A.Z. Amanci, F.P. Dawson, and H.E. Ruda, "Galvanic isolation for high frequency applications using an integrated dielectric structure," in *IEEE ECCE*, Sep- 15–19, 2013, pp. 3726—3732.
[7] M.H. Rashid, *Power Electronics Handbook*, B-H Elsevier, 2011.
[8] R. Hou, P. Magne, B. Bilgin and A. Emadi, "A topological evaluation of isolated DC/DC converters for Auxiliary Power Modules in Electrified Vehicle applications," in *IEEE APEC*, Mar. 15–19, 2015, pp. 1360-1366.
[9] L. Roggia, F. Beltrame, L. Schuch and J. R. Pinheiro, "Comparison between full-bridge-forward converter and DAB converter," in *IEEE COBEP*, Oct. 27–31, 2013, pp. 224–229.
[10] G.T. Chiang, T. Sugiyama, and M. Sugai, "Consideration of PDM and power decoupling method in an isolated single-phase matrix converter for battery charger," *Review of Toyota CRDL*, vol. 48, No. 2, pp. 11–19, May, 2017.
[11] M.H. Rashid, *Power Electronics Circuits Devices: Devices, Circuits, and Applications*, Prentice Hall–Pearson, 2014.
[12] M. Valco, P. Sindler, J. Sedo and J. Kuchta, "Inverter output voltage under different type of loads," in *IEEE ELEKTRO*, May 19–20, 2014, pp. 383-388.
[13] M. Hasan, J. Maqsood, M.Q. Baig, S.M. Bukhari and S. Ahmed, "Design and Implementation of Single Phase Pure Sine Wave Inverter Using Multivibrator IC," in *IEEE UKSim*, Mar. 25–27, 2015, pp. 451–455.
[14] P.W. Wheeler, J.C. Clare, L. Empringham, M. Bland and K.G. Kerris, "Matrix converters," *IEEE Ind. Appl. Mag.*, vol. 10, no. 1, pp. 59–65, 2004.
[15] R. Ortega, A. Loria, P.J. Nicklasson, and H. Sira-Ramirez, *Passivity-Based Control of Euler–Lagrange Systems*. New York: Springer-Verlag, 1998.